

Analysis of Electrolytes and Fluid Volumes Disturbances during Hyperglycemia-Induced Hyponatremia in Diabetes Mellitus Type 1

Mohammed Ferdjallah^{1*}, Asad Salem², Zeid Khitan³ and Henry Driscoll³

¹ Department of Computer Science & Electrical Engineering, Marshall University, USA

² Department of Mechanical Engineering, Marhsall University, USA

³ Department of Internal Medicine, Marshall University Joan C. Edwards School of Medicine, USA

Review Article

*Corresponding author

Mohammed Ferdjallah,
Department of Computer Science &
Electrical Engineering,
Department of Biomedical
Engineering, College of Engineering &
Computer Science, Weisberg Applied
Engineering Complex, Suite 3105,
Marshall University, Huntington,
WV 25755,

Email: ferdjallah@marshall.edu

Article Information

Received: 09 Sep 2024;
Accepted: 13 Sep 2024;
Published: 20 Sep 2024.

Abstract

The objective of this study is to investigate the effects of hypovolemia on hyperglycemia-induced hyponatremia in diabetes mellitus type 1 (DMT1). Because of the change in osmolarity due to increased serum glucose, the serum sodium concentration may be relative and may not reflect the actual concentration of sodium. Although it has been accepted that serum sodium must be corrected by a factor of 1.6 during hyperglycemia-induced hyponatremia, recent studies suggest that the correction factor is much higher when serum glucose is higher than 400 mg/dL. In this study we designed a state-based model to provide a generalized approach to the correction factor of serum sodium when hypovolemia occurs in high serum glucose in chronic or uncontrolled hyperglycemia in DMT1. In this simulation study, we demonstrated that the intravenous (IV) injection of 1000 mOsm glucose bolus cause rapid fluid shift among the body fluid compartments. This fluid shift momentarily causes an expansion of the Extracellular Fluid (ECF) and the Intracellular Fluid (ICF) fluid compartments. However, after rapid glucose metabolism, some of the plasma fluid will be excreted when the kidney absorptive capacity is exceeded. The initial loss of water from the plasma fluid compartment will be redistributed among the body fluid compartments by the effect of osmosis. This fluid redistribution relatively reduces the effective fluid loss from the plasma fluid compartments, which in turn causes the loss of electrolytes proportionally. The overall loss of fluid not only causes contraction of plasma fluid but also contraction of ICF. A correction factor for sodium may be as high as 5.5 at high Hemoglobin A1c (HbA1c) levels. Hyperglycemia causes electrolytes and fluids disturbances that can be predicted using state-based modeling and simulation models using a data-based empirical function of insulin resistance/insufficiency at a priori HbA1c level.

Keywords: Electrolytes; Diabetes Mellitus Type 1; Hypovolemia; Correction Factor; Hyperglycemia-Induced Hyponatremia

Glossary	
ECF	Extracellular fluid (L)
ICF	Intracellular fluid (L)
ICFI	Intracellular fluid of insulin insensitive tissues (L)
ICFS	Intracellular fluid of insulin sensitive tissues (L)
$[G]_{si}$	Glucose concentration in state s_i (mg/dL)

Citation: Ferdjallah M, Salem A, Khitan Z, Driscoll H; Analysis of Electrolytes and Fluid Volumes Disturbances during Hyperglycemia-Induced Hyponatremia in Diabetes Mellitus Type 1. Medp Public Health Epidemiol. 2024; 4(1): mpphe-202409001.

$[G]_{Th}$	Glucose concentration threshold of the kidney (mg/dL)
G_t	Glucose bolus (mOsm)
G_{si}	Glucose content in state s_i (mOsm)
G_{si}^{ecf}	Glucose content of ECF in state s_i (mOsm)
G_{si}^{icfi}	Glucose content of ICFI in state s_i (mOsm)
G_{excess}	Excess glucose in state s_i (mOsm)
$G_{excreted}$	Excreted glucose by the kidney (mOsm)
G_{t-si}	Total glucose in state s_i (mOsm)
$[Na^+]_{si}$	Potassium concentration in state s_i (mEq/L)
$[Na^+]_{si}$	Sodium concentration in state s_i (mEq/L)
$Na^+_{excreted}$	Sodium content excreted (mEq)

$\eta_{[Na^+]}$	Sodium concentration correction factor
$\eta_{[K^+]}$	Potassium concentration correction factor
O_{si}	Osmolarity in state s_i (mOsm/L)
$V_{excreted}$	Fluid volume excreted (L)
V_{si}^{ecf}	Fluid volume of ECF in state s_i (L)
V_{si}^{icfi}	Fluid volume of ICFI in state s_i (L)
V_{si}^{icfs}	Fluid volume of ICFS in state s_i (L)
$V_{si}^{ecf-shift}$	Fluid volume shift to or from ECF in state s_i (L)
$V_{si}^{icfi-shift}$	Fluid volume shift to or from ICFI in state s_i (L)
V_{si}^t	Total fluid volume in state s_i (L)
TBW	Total body water (L)

Introduction

Currently, there are 1.6 million patients with Diabetes Mellitus Type 1 (DMT1) in the USA and more than 460 million worldwide [1-3]. In the USA, the health cost associated with DMT1 was estimated to be more than \$325 billion in 2017 [4,5]. When managed properly, a patient with DMT1 can live a normal life. The average life expectancy of patient with DMT1 is currently 66 and 68 years for men and women respectively [6-8]. Although, DMT1 is considered sporadic with low heritance risk, environmental conditions have significance impact on genetically predisposed patients when exposed to infections that provoke autoimmune reactions. Consequently, DMT1 results from the chronic autoimmune destruction of beta cells of the pancreas [9-11]. DMT1 is typically diagnosed in childhood after a viral infection or an inflammatory condition. Treatment of DMT1 is a lifelong daily injection of exogenous insulin. Long term complications of DMT1 include retinopathy, neuropathy, nephropathy, cardiovascular diseases, and dementia [12-20]. In poorly managed DMT1, ketoacidosis can occur, and if left untreated it may lead to brain edema, brain injury, and rarely death [21-26]. Nonetheless, despite advance in management and treatment, death from ketoacidosis is still a potential risk [27-29].

Uncontrolled increase of serum glucose level is associated with decrease serum sodium concentration. This hyperglycemia-induced hyponatremia is caused by cyclic attempts of the body to compensate for the continuous loss of water and electrolytes

[30-32]. Because of the uptake of glucose by some tissues is insulin sensitive, the equilibrium of glucose concentration is not uniform throughout the body. Consequently, fluid will shift between the body compartments to maintain serum osmolarity close to normal as much as possible [33-36]. This fluid shift will inevitably change the concentration of serum electrolytes [37,38]. Although the kidneys will attempt to maintain glucose homeostasis, a correcting for electrolytes and water is necessary to maintain important bodily functions [39,40]. The correction by a factor of 2.8, as predicted by the body volume compartments proportionality, has been shown to be appropriate when glucose concentration exceeds 400 mg/dL [41]. Earlier on, Katz demonstrated that a factor of 1.6 would be enough in acute changes of serum glucose [42]. Others have suggested more tight correction factors to account for metabolic effects of insulin sensitive and insulin non-sensitive tissues [43]. The objective of this study was to investigate serum electrolytes disturbances in patients with DMT1 during severe hyperglycemia. Thus, the overall specific aim of this study was to demonstrate through simulation that the sodium concentration correction factor is much higher than that estimated by Katz's study.

The purpose of this simulation is to better understand the effects of hyperglycemia on electrolytes and fluid volumes, as well as how these changes contribute to the risks of diabetic ketoacidosis and cerebral edema. Although the effects of hyperglycemia on brain edema are not fully understood,

Citation: Ferdjallah M, Salem A, Khitan Z, Driscoll H; Analysis of Electrolytes and Fluid Volumes Disturbances during Hyperglycemia-Induced Hyponatremia in Diabetes Mellitus Type 1. Medp Public Health Epidemiol. 2024; 4(1): mpphe-202409001.

increased glucose has definite effects on fluid volumes and electrolytes and thus has many ways that may lead to neuronal damage especially in the hippocampus. It has been established that increase serum glucose causes direct damage on small vessels [44-46]. In addition, hyperglycemia has been associated with fluid volume and electrolytes loss [47-48]. Imbalance in fluid volumes and electrolytes stimulates autoregulation in sensitive tissues such as the brain, which may lead to brain edema or brain tissues shrinking [49]. Therefore, a critical review of the effects of increased serum glucose on body fluid volume compartments and electrolytes is warranted. This simulation addresses three main specific aims. The first aim is to investigate the extent of volume loss during hyperglycemia. The second aim is to investigate how and where glucose accumulates. The third aim is to investigate whether maintaining fluid and electrolytes balance could be a potential intervention for reducing the risks of diabetic ketoacidosis and brain edema. In this study, we will focus on the patients with DMT1. We propose a generalized approach that will account for the effects of hypovolemia induced by the chronic elevated serum glucose using state-based modeling and simulation models using a data-based empirical function of insulin resistance/insufficiency at a priori hemoglobin A1c (HbA1c) level. The rationale of using HbA1c instead of measured blood glucose is to incorporate the capacity of the pancreas through a sigmoid function model described by experimental data.

Methodology

The objective of this study was to investigate serum electrolytes disturbances in patients with DMT1 during severe hyperglycemia. For emergency interventions of severe hyperglycemia, quasi-stable state model is most appropriate when vital signs can be assessed through immediate measurements. In normal management, a patient with DMT1 is currently accomplished using daily application of insulin or automated insulin delivery systems. Thus, under these management conditions, patients with DMT1 should not fall into severe hyperglycemia and ketoacidosis when these systems are working properly. However, when these patients spiral into serious conditions, they are usually admitted and managed by aggressive fluid resuscitation and insulin injection. In the next sections, we describe the design of this simulation study using a quasi-stable state model. The model represents the accumulation, absorption, and excretion of excess glucose following the action of exogenous insulin and kidney fluid regulation in patients with DMT1. We used reference values for body fluid compartments volumes and serum electrolytes used by Katz to allow for comparison (Table 1). In section 2.1, we described an HbA1c-varying state model that governs the transitions of the simulation. In section 2.2, we described the normal glucose metabolism and state Katz's basis for serum electrolytes concentrations correction. In section 2.3, we described how glucose is accumulated, absorbed, and excreted in patients with DMT1 using a state-based model to infer correction factors for serum electrolytes concentrations. We used the notation $[*]$ to indicate concentration of a solute and the notation V_{sub}^{sup} to indicate its associated volume. The superscript refers to the compartment, and the subscript refers to the state of the model. For the mass of a solute, we used the term "content" instead of the term "mass". Finally, we listed the assumptions of the model in Table 2.

Table 1: Normal body fluid compartments volumes and serum electrolytes concentration reference values. Fluid compartments include TBW (total body water), ICFS (intracellular fluid of insulin sensitive tissues), ICFI (intracellular fluid of insulin insensitive tissues), ECF (extracellular fluid), ISF (interstitium fluid), and PF (plasma fluid).

Body fluid compartments volumes		Serum Electrolytes	
TBW(L)	42	Sodium (mEq/L)	140
ICFS(L)	23	Potassium (mEq/L)	4.5
ICFI(L)	5	Glucose (mg/dL)	90
ECF(L)	14	BUN (mg/dL)	15
ISF(L)	11	Creatinine (mg/dL)	1.05
PF(L)	3	Calcium (mg/dL)	9.5

Table 2: The list of the main assumptions of the model.

Model Assumptions
<ul style="list-style-type: none">• All body fluid compartments, and concentrations values used are adapted from published references.• The model has only one cycle of 5 hours, which represents the duration of the diagnostic glucose challenge test.• The insulin resistance/insufficiency function was designed using published Matsuda index data.• Kidney glucose threshold function was designed using published data.• The complete blood osmolarity that includes sodium, potassium, glucose, and blood urea nitrogen (BUN) was used.• The model starts immediately after the injection of 1000 mOsm intravenous (IV) glucose bolus.• The insulin resistance/insufficiency function simulates the glucose that can enters the intracellular fluid of insulin sensitive tissues (ICFS).• The IV glucose bolus is the main source of glucose. No other source of glucose is considered.

HbA1c-Varying Model Design

Glucose metabolism is accomplished through many mechanisms that take place concurrently. Membrane proteins (glucose transporters, GLUTs) govern cellular glucose absorption, some of which are integrated into the cell membrane by the action of insulin. Sodium dependent glucose transporters (S-GLUT) regulate cellular glucose uptake in the gut and kidney. Normally, glucose uptake is accomplished by insulin-sensitive and insulin-insensitive tissues [50]. However, in patients with DMT1, glucose metabolism depends mostly on exogenous insulin intake in severe hyperglycemia because glucose uptake by insulin-insensitive tissues is not enough to manage the patient. In this case, abnormal glucose metabolism may occur despite therapeutic management. Any excess glucose that was not used by insulin sensitive tissues may accumulate in ECF due to either insulin resistance or insulin insufficiency. The excess glucose beyond the absorptive capacity of the kidney may be excreted in the urine pulling equivalent water and electrolytes with it. Normally, a patient with DMT1 is managed with a regimen of exogenous insulin to maintain an HbA1c level under 7.0. However, HbA1c level can be elevated in a poorly managed patient due to either insulin resistance or insufficiency.

To assess the dynamics of body fluid compartments volumes and serum electrolytes, we designed a state model that represents the effects of insulin action and kidney fluid regulatory mechanisms. Mathematical models of glucose metabolism are based on differential equations that describe the dynamics of

glucose and insulin feedbacks to regulate blood glucose [51,52]. These models have several parameters and depend on initial and boundary conditions with many assumptions that may not be accurate during severe hyperglycemia and ketoacidosis. These models are often implemented by numerical models and require complex computational systems. In addition, the differential equation modeling assumes dynamic perturbations around an equilibrium level to maintain homeostasis, which may not be possible under these conditions. For emergency interventions of severe hyperglycemia, quasi-stable state model is most appropriate when vital signs can be assessed through immediate measurements. In this study, we propose a model that represents an expansion of Katz's study, in which we defined quasi-stable independent states representing the actions of insulin and the kidney. Katz's model describes body volume changes before and after the IV injection of glucose bolus.

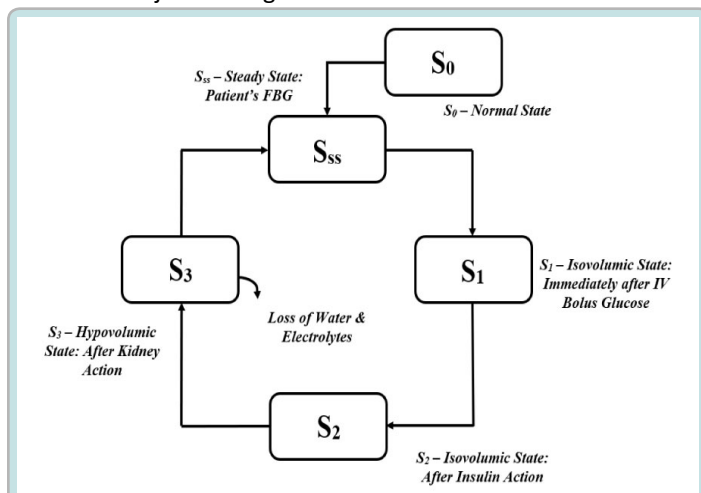


Figure 1: State model for the simulation of hyperglycemia effects on body fluid compartments volumes and serum electrolytes concentrations. The functional state model consists of five quasi-stable states S_{ss} , S_0 , S_1 , S_2 , and S_3 . S_{ss} represents the steady state of the patient's fasting blood glucose. S_0 represents the steady state before the injection of IV glucose bolus. S_1 represents the isovolumic state immediately after IV injection of glucose bolus and before the action of insulin and the kidney. S_2 represents the isovolumic state after the action of insulin. S_3 represents the hypovolemic state after the action of the kidney and the loss of water and electrolytes.

Figure 1 illustrates a functional state model that consists of six quasi-stable states S_{ss} , S_0 , S_1 , S_2 , and S_3 . S_{ss} represents the steady state of the patient's fasting blood glucose. S_0 represents the steady state before the injection of IV glucose bolus. S_1 represents the isovolumic state immediately after IV injection of glucose bolus. S_2 represents the isovolumic state after the action of insulin. S_3 represents the hypovolemic state after the action of the kidney and the loss of water and electrolytes. These states represent the body fluid compartments volumes before and after the infusion of IV glucose bolus during one cycle of simulation. We define a cycle of simulation as a period of 5 hours, which represents the time allocated to perform the diagnostic glucose tolerance test. During a cycle no glucose or fluids is added to the body system. In addition, we assume that no endogenous glucose is generated during a simulation cycle. The model simulates glucose uptake by insulin sensitive tissues as a function of insulin resistance/insufficiency. Furthermore, we assume the action of insulin is faster than that of the kidney. For instance, when the system is in state S_1 , neither state S_2 nor state S_3 are

activated. When the system transitions from state S_1 , it would move to state S_2 before moving to state S_3 and so on. Similar to Katz's model, the rationale of assuming steady states is to assist health care providers to predict emergency clinical interventions during severe hyperglycemia and ketoacidosis based on patients measured vital data. Although patients with DMT1 are generally managed with exogenous insulin to maintain an HbA1c level under 7.0, to illustrate poor management or poor compliance, the simulation model allows levels of HbA1c ranging from 4.0 to 9.0. At high levels of HbA1c the risks for ketoacidosis can lead to severe complications.

Several studies investigated the correlation between insulin secretion and beta cell mass [53-56]. In DMT1, beta cells mass is negligible; however, when managed properly with exogenous insulin, patients with DMT1 would have an equivalent of 100% of beta cell mass with a full apparent function. Therefore, an exogenous dose of insulin, whether appropriate or not, would represent an equivalent percent of beta cells mass that secretes the same content of insulin. Matsuda index represents the ability of beta cells to secrete insulin and maintain an HbA1c level that corresponds to the fasting blood glucose of the patient. The Matsuda index is an empirical expression that relates insulin and glucose levels during an oral glucose tolerance test with five measurements at 0, 30, 60, 90 and 120 min. Thus, the Matsuda index represents the functional ability of beta cell mass to secrete the corresponding level of insulin. We used published studies that relates Matsuda index to HbA1c level to design a normalized empirical function, $f(h)$, to simulate beta cell mass. The function $f(h)$ represents the percent insulin resistance/insufficiency as a function of HbA1c level, which is denoted by h . The function $f(h)$ is a unit function derived from an inverted normalized Matsuda index curve generated in reference [57]. The function $f(h)$ can be approximated by an expression, which is regulated by a mass dependent process of beta cells [58]. The function $f(h)$ is expressed as follows:

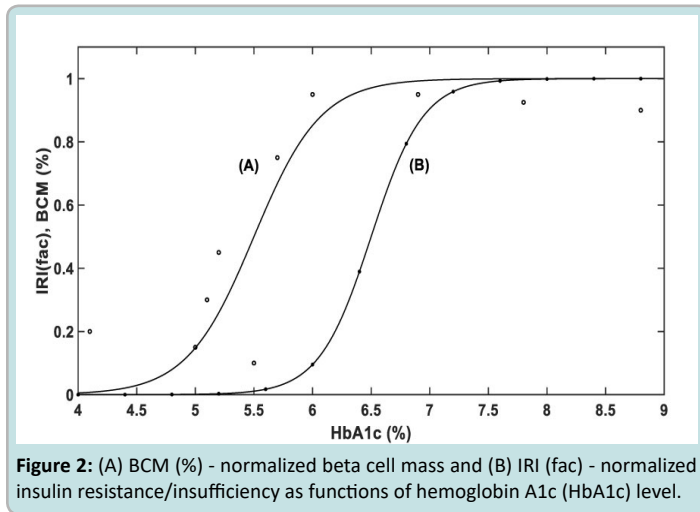
$$f(h) = \frac{K_0}{1 + Q_0 \exp(-r(h - h_0))} \quad \text{---- (1)}$$

Equation 1 represents a nonlinear relationship between HbA1c level, and the percent of beta cells mass as depicted in Figure 2(A). The least square method based on the modified Newton criterion was used to estimate the parameters of Equation 1 [59,60]. The parameters of Equation 1 are estimated as $K_0 = 0.9$, $Q_0 = 0.3$, $r = 1.5$, and $h_0 = 6.5$. To simulate the association between HbA1c level and function of beta cells, we assumed that insulin resistance/insufficiency is reduced to half (50% decrease in beta cells' function), when there is a loss of nearly 90% of beta cells mass, which occurs around an HbA1c level of 7.0. Insulin resistance/insufficiency can be represented by the function $f(h)$ but with a shift parameter h_0 equal to 7.0 as illustrated by Figure 2(B). In the case of insulin resistance, beta cell function may not change; however, peripheral tissue resistance to insulin would result in an apparent functional decrease in beta cells. Therefore, Equation 1 can also be used for insulin resistance.

Normal Glucose Metabolism

To infer associations between changes in body fluid compartments and serum increased glucose, we will use the state model described in Figure 1 that represents the equilibrium conditions before and after glucose metabolism following the IV injection of glucose bolus. We denote the Total Body Water (TBW),

Intracellular Fluid (ICF), Extracellular Fluid (ECF), Interstitium Fluid (ISF), and plasma fluid (PF) by V^t , V^{icf} , V^{ecf} , V^{isf} , and V^{pf} respectively. To account for the insulin-sensitive and insulin sensitive tissues, we divided the intracellular volume into two volumes (ICFI, ICFS) representing the insulin-insensitive and insulin-sensitive tissues and denoted by V^{ICFI} and V^{ICFS} respectively. Insulin-sensitive tissues require insulin to uptake glucose, whereas insulin-insensitive tissues do not. We also divided the extracellular volume into ISF and PF representing the interstitium fluid and plasma fluid. We also denote the serum osmolarity, serum glucose, and serum blood urea nitrogen (BUN) by O , G , and U , respectively. Just before the IV injection of the glucose bolus, the serum osmolarity is expressed as follows:



$$O_{s0} = 2[Na^+]_{Serum} + 2[K^+]_{Serum} + \frac{1}{18}[G_{Serum}] + \frac{1}{2.8}[U_{Serum}] \quad (2)$$

Where $[Na^+]$, $[K^+]$, $[G_{Serum}]$, $[U_{Serum}]$ are the concentrations of sodium, potassium, serum glucose, and serum blood urea nitrogen (BUN) respectively. The constants 2, 1/18, and 1/2.8 represent the effective osmoles (i.e., dissolved particles) of Na^+ , K^+ , glucose, and BUN in the blood respectively. When glucose increases beyond the steady state value, serum osmolarity will change to accommodate the inability of glucose to normalize rapidly between body fluid compartments. With the addition of an IV glucose bolus (G_b) (in mOsm) to ECF, the new serum osmolarity is expressed as follows:

$$O_{s1} = \frac{1}{V_{s1}}(O_{s0} V_{s0} + G_b) \quad (3)$$

S_1 is the state representing the body fluid compartments just after the IV glucose bolus. From Equation 3, the serum osmolarity will increase as the serum glucose increases. Similar to Katz study, we will assume that glucose content of ICFS is negligible. Consequently, fluid will move from ICFS to ECF and ICFI to accommodate for the increase in osmolarity due to the addition of the IV glucose bolus. The portion of fluid shift to ECF is expressed as follows:

$$V_{S1}^{ecf-shift} = (V_{S0}^{icfs} - V_{S1}^{icfs}) \left(\frac{V_{S0}^{ecf}}{V_{S0}^{ecf} + V_{S0}^{icfi}} \right) \quad (4a)$$

$$V_{S1}^{ecf-shift} = V_{S0}^{icfs} \left(1 - \frac{O_{S0}}{O_{S1}} \right) \left(\frac{V_{S0}^{ecf}}{V_{S0}^{ecf} + V_{S0}^{icfi}} \right) \quad (4b)$$

Similarly, the portion of fluid shift to ICFI is expressed as follows:

$$V_{S1}^{icfi-shift} = V_{S0}^{icfs} \left(1 - \frac{O_{S0}}{O_{S1}} \right) \left(\frac{V_{S0}^{icfi}}{V_{S0}^{ecf} + V_{S0}^{icfi}} \right) \quad (5)$$

Due to this fluid volume shift, the new ECF and ICFI volumes will then be updated and expressed as follows:

$$V_{S1}^{ecf} = V_{S0}^{ecf} + V_{S1}^{ecf-shift} \quad (6a)$$

$$V_{S1}^{icfi} = V_{S0}^{icfi} + V_{S1}^{icfi-shift} \quad (6b)$$

Since there is not fluid excretion yet, the increase in fluid content in ECF and ICFI does not change the total body water content. However, the change in body fluid volumes will increase or decrease electrolytes concentrations proportionally to the fluid shift. In particular, the new ECF concentration of sodium can be expressed as follows:

$$[Na^+]_{S1} = [Na^+]_{S0} \left(\frac{V_{S1}^{ecf}}{V_{S0}^{ecf}} \right) \quad (7)$$

Consequently, the serum sodium concentration change, with respect to the steady state sodium concentration, will be expressed as follows:

$$[Na^+]_{S1} - [Na^+]_{S0} = [Na^+]_{S0} \left(\frac{V_{S1}^{ecf}}{V_{S0}^{ecf}} - 1 \right) \quad (8)$$

According to Katz, this change in serum sodium concentration can be proportionally correlated with the change in serum glucose, which is expressed as follows:

$$G_{S1} - G_{S0} = \frac{[G]_{S1} - [G]_{S0}}{18} \quad (9)$$

The relationship between the change in serum sodium concentration (Equation 8) and blood glucose concentration (Equation 9) is established indirectly by the estimated water shift from ICF to ECF. This relationship is established theoretically through proportionality principle. The relationship has been used to estimate a correction to the measured serum sodium when the change in blood glucose is known. It is expressed as follows:

$$[Na^+]_c - [Na^+]_m = \frac{[1.6]}{100} ([G]_m - 100) \quad (10)$$

$[Na^+]_c$ is the corrected serum sodium concentration, $[Na^+]_m$ is the measured serum sodium concentration, and $[G]_m$ is the measured serum glucose concentration in (mg/dL). The normal glucose reference level was considered equal to 100 (mg/dL). The constant 1.6 was clinically termed the "correction factor". For each 100 mg/dL increase of glucose above 100 mg/dL, sodium concentration increases by a factor of 1.6 mEq/L. In normal individuals, with functioning pancreas and kidney, the correction factor is equal to 0. The interpretation of the relationship, in Equation 10, has been conflicting and has been used indiscriminately. Proving the clinical validity of this expression does not seem to be possible yet. The connection of this expression to disruptions in glucose metabolism is not as trivial. According to Katz's original expression, the addition of glucose bolus directly into the ECF would cause an immediate fluid shift from the insulin sensitive tissues of ICF fluid into ECF. In the total absence of insulin action, this assumption may be relatively accurate. However, in the presence of insulin action, the glucose injected in ECF will be driven into insulin sensitive tissues, and the fluid shifted into ECF will be reversed and serum electrolytes balance will be re-established.

Abnormal Glucose Metabolism in DMT1

In patients with DMT1, glucose metabolism depends solely on exogenous insulin intake. In this case abnormal glucose metabolism may occur despite therapeutic management. Any excess glucose that was not used by insulin sensitive tissues may accumulate in ECF due to either insulin resistance or insulin insufficiency. State S_1 represents the body fluid compartments just after the IV glucose bolus. During state S_1 , after the addition of IV glucose bolus (mOsm) into ECF, the total body glucose (mOsm) and the ECF glucose (serum) are expressed as follows:

$$G_{S1}^t = G_b + \frac{1}{18} [G]_{S0} (V_{S0}^{ecf} + V_{S0}^{icfs}) \quad \text{---- (11a)}$$

$$G_{S1}^{ecf} = G_b + \frac{1}{18} [G]_{S0} V_{S0}^{ecf} \quad \text{---- (11b)}$$

We assume there is a negligible glucose in insulin sensitive tissues (ICFS) prior to the addition of the IV glucose bolus in ECF. The new osmolarity denoted by O_{S1} (Equation 3) is due to the addition of the IV glucose bolus G_b . This change in osmolarity will cause immediate shift of fluid among ICFS, ICFI, and ECF volumes as shown by Equations 4 through 6. Insulin insensitive tissues readily uptake glucose without the need for insulin and thus ICFI increases as fluid follows glucose. Once the IV glucose bolus is administered, an IV insulin dose is also administered. The dose of insulin is selected to maintain a fasting blood glucose that corresponds to the HbA1c level of the patient. The state S_2 represents the state of the body fluid compartments after the action of insulin followed by the action of the kidney. Immediately after the action of insulin, and assuming that there is no significant influx of glucose from either the liver or the kidney, the content of glucose that is consumed by insulin-sensitive tissues of ICFS is expressed as follows:

$$G_{S2}^{icfs} = (1 - f(h)) G_b \frac{V_{S1}^{icfs}}{V_{S0}^t} \quad \text{---- (12)}$$

The function $f(h)$, illustrated in Figure 1, represents the percent insulin resistance/insufficiency as a function of HbA1c, which is denoted by h . The function $f(h)$ can be approximated by an expression, which is regulated by a mass dependent process of beta cells as described by Equation 1. We assume that insulin resistance/insufficiency is proportional to the excess content of glucose that was not utilized by the insulin sensitive tissues. Under normal osmolar equilibrium, the IV glucose bolus will distribute in body fluid volume compartments as such that the contents of glucose in ECF and ICFI are expressed as follows:

$$G_{S2}^{icfs} = G_b \frac{V_{S1}^{icfs}}{V_{S0}^t} \quad \text{---- (13a)}$$

$$G_{S2}^{ecf} = G_b \frac{V_{S1}^{ecf}}{V_{S0}^t} \quad \text{---- (13b)}$$

In the beginning of state S_2 , the fraction of the added glucose that was supposed to be absorbed by insulin sensitive tissues is expressed as follows:

$$G_{S2}^{excess} = f(h) G_b \frac{V_{S1}^{icfs}}{V_{S0}^t} \quad \text{---- (14)}$$

Equation 14 represents the portion of glucose that remains in ECF and is redistributed proportionally between ECF and ICFI. In the process of glucose uptake by insulin-sensitive tissue, there is a decrease in serum glucose level, with respect to the initial glucose bolus. The new total glucose and ECF glucose (serum) are expressed as follows:

$$G_{S2}^t = G_{S1}^t \left[1 - (1 - f(h)) \frac{V_{S1}^{icfs}}{V_{S0}^t} \right] \quad \text{---- (15a)}$$

$$G_{S2}^{ecf} = G_{S1}^{ecf} \left[1 - (1 - f(h)) \frac{V_{S1}^{icfs}}{V_{S0}^t} \right] \quad \text{---- (15b)}$$

A portion of the excess of glucose in ECF will be excreted through the kidney when the glucose concentration exceeds the glucose absorptive capacity of the kidney. In normal individuals, the glucose absorptive capacity of the kidney is around 180 mg/dL, whereas in diabetic patients, the glucose absorptive capacity is between 180 and 220 mg/dL [61-63]. We model the glucose threshold of the kidney, denoted by $[G]_{thr}$, as a sigmoid function of HbA1c paralleling the insulin resistance/insufficiency and increasing from 180 mg/dL to 220 mg/dL as illustrated in Figure 3. Therefore, the glucose threshold is expressed as follows:

$$[G]_{thr} = 180 + 40 f(h) \quad \text{---- (16)}$$

The ECF glucose (serum) remains the same as expressed in Equation 15b if the serum glucose does not exceed the glucose

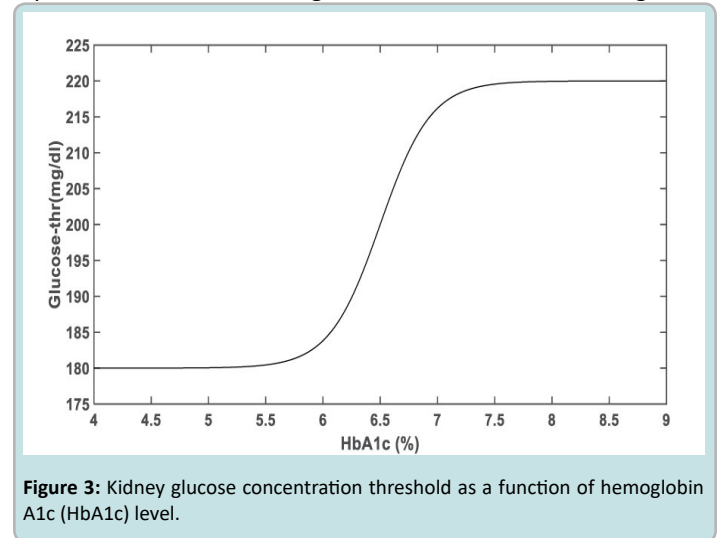


Figure 3: Kidney glucose concentration threshold as a function of hemoglobin A1c (HbA1c) level.

threshold of Equation 16. On the other hand, if ECF glucose exceeds that of the absorptive capacity of the kidney, a portion of excess ECF glucose will be excreted through the kidney. Assuming normal linear kidney clearance, the total glucose excreted by the kidney can be estimated by the following expression as follows:

$$G_{excreted} = ([G]_{S2}^{ecf} - [G]_{thr}) V_{S2}^{ecf} \quad \text{---- (17)}$$

In the process of glucose excretion by the kidney action, there is a decrease in serum glucose level, with respect to the initial glucose bolus. The new total glucose is expressed as follows:

$$G_{S3}^t = G_{S1}^t \left[f(h) \frac{V_{S1}^{icfs}}{V_{S0}^t} \right] - G_{excreted} \quad \text{---- (18a)}$$

$$G_{S3}^{ecf} = G_{S1}^{ecf} \left[f(h) \frac{V_{S1}^{icfs}}{V_{S0}^t} \right] - G_{excreted} \quad \text{---- (18b)}$$

The portion of excreted glucose will pull fluid (mainly water) with it due to osmotic effect. The fluid volume excreted with the excreted glucose is expressed as follows:

$$V_{excreted} = 18 \frac{G_{excreted}}{[G]_{S2}^{ecf}} \quad \text{---- (19)}$$

The excreted fluid volume will cause an additional fluid loss from the total body water. The new total body water is then expressed as follows:

$$V_{S3}^t = V_{S2}^t - V_{\text{excreted}} \quad \text{--- (20)}$$

The fraction of glucose absorbed by insulin-sensitive tissues will cause rebalancing of water among ICFI, ICFS, and ECF volumes and creates a new state of body fluid compartment denoted by S_3 . The decrease in total glucose due to insulin-sensitive uptake will cause change in osmolarity and redistribution of fluid volumes. With this decrease in serum glucose, there will be some fluid shift back to ICFS from ICFI and ECF, which were estimated by Equations 4 through 6. Consequently, the new total contents of glucose found in ICFI and ECF are expressed as follows:

$$G_{S3}^{\text{ecf}} = G_{S3}^t \left(\frac{V_{S2}^{\text{ecf}}}{V_{S2}^{\text{ecf}} + V_{S2}^{\text{icfi}}} \right) \quad \text{--- (21a)}$$

$$G_{S3}^{\text{icfi}} = G_{S3}^t \left(\frac{V_{S2}^{\text{icfi}}}{V_{S2}^{\text{ecf}} + V_{S2}^{\text{icfi}}} \right) \quad \text{--- (21b)}$$

The excess of glucose in ECF, after insulin-sensitive tissues uptake, causes a resultant fluid shift (with respect to steady state conditions) from ICFS to ECF and ICFI. According to Equation 4b, the resultant fluid shift associated with the excess glucose in ECF is expressed as follows:

$$V_{S3}^{\text{ecf-shift}} = V_{S0}^{\text{icfs}} \left(1 - \frac{0_{S0}}{0_{S2}} \right) \left(\frac{V_{S0}^{\text{ecf}}}{V_{S0}^{\text{ecf}} + V_{S0}^{\text{icfi}}} \right) \quad \text{--- (22a)}$$

$$V_{S3}^{\text{ecf-shift}} = V_{S0}^{\text{icfs}} \left(\frac{G_{S2}^{\text{t-new}}}{0_{S2} V_{S0}^t + G_{S2}^{\text{t-new}}} \right) \left(\frac{V_{S0}^{\text{ecf}}}{V_{S0}^{\text{ecf}} + V_{S0}^{\text{icfi}}} \right) \quad \text{--- (22b)}$$

Similarly, and according to Equation 5, the portion of fluid shift in ICFI is expressed as follows:

$$V_{S3}^{\text{icfi-shift}} = V_{S0}^{\text{icfs}} \left(\frac{G_{S2}^{\text{t-new}}}{0_{S2} V_{S0}^t + G_{S2}^{\text{t-new}}} \right) \left(\frac{V_{S0}^{\text{icfi}}}{V_{S0}^{\text{ecf}} + V_{S0}^{\text{icfi}}} \right) \quad \text{--- (22c)}$$

Due to the resultant fluid shift, the new ECF and ICFI volumes will then be expressed as follows:

$$V_{S3}^{\text{ecf}} = V_{S0}^{\text{ecf}} + V_{S3}^{\text{ecf-shift}} \quad \text{--- (23a)}$$

$$V_{S3}^{\text{icfi}} = V_{S0}^{\text{icfi}} + V_{S3}^{\text{icfi-shift}} \quad \text{--- (23b)}$$

The active uptake of glucose by insulin-sensitive tissues and the passive insulin-insensitive tissues uptake should allow serum glucose to return to steady state level. Normally, when cellular activity is maintained by sufficient glucose, the kidney will remove the excess glucose. Assuming that the glucose in ICFS is negligible due to insulin dependent cellular metabolism, the total new glucose equilibrium content (mainly in ECF and ICFI) produces a concentration that is expressed as follows:

$$[G]_{S3} = 18 \frac{G_{S3}^t}{V_{S3}^{\text{ecf}} + V_{S3}^{\text{icfi}}} \quad \text{--- (24)}$$

Consequently, the glucose content in ECF is expressed as follows:

$$G_{S3}^{\text{ecf}} = \frac{1}{18} [G]_{S3} V_{S3}^{\text{ecf}} \quad \text{--- (25)}$$

The excreted fluid will also pull with its electrolytes proportional to the adjusted excreted ECF volume after body fluids redistribution as expressed in Equations 22a-c. In particular, the content of sodium that is excreted in the urine, with respect to the steady state, is expressed as follows:

$$Na_{\text{excreted}}^+ = [Na^+]_{S0} V_{\text{excreted}} \quad \text{--- (26)}$$

The new sodium concentration after ECF volume contraction is expressed as follows:

$$[Na^+]_{S3} = \frac{[Na^+]_{S0} V_{S0}^{\text{ecf}} - Na_{\text{excreted}}^+}{V_{S3}^{\text{ecf}}} \quad \text{--- (27)}$$

The change in serum sodium concentration is expressed as follows:

$$[Na^+]_{S3} - [Na^+]_{S0} = [Na^+]_{S0} \left(\frac{V_{S0}^{\text{ecf}} - V_{\text{excreted}}}{V_{S3}^{\text{ecf}}} - 1 \right) \quad \text{--- (28)}$$

We will attempt to relate this change in serum sodium concentration to the change in serum glucose according to Katz's Equation 10, which considers the change of glucose as the difference between the glucose level after the IV glucose bolus and fasting blood glucose expressed in concentration units (mg/dL). Since the current sodium and glucose concentrations can be estimated in state S_3 by Equations 25, 26, and 27, a correction factor for the sodium concentration can be expressed as follows:

$$\eta_{[Na^+]} = [G]_{ss} \frac{[Na^+]_{S3} - [Na^+]_{ss}}{[G]_{S3} - [G]_{ss}} \quad \text{--- (29)}$$

A similar expression can be derived for the correction factor of the potassium concentration as follows:

$$\eta_{[K^+]} = [G]_{ss} \frac{[K^+]_{S3} - [K^+]_{ss}}{[G]_{S3} - [G]_{ss}} \quad \text{--- (30)}$$

Equations 29 and 30 estimate the proportionality factors between the change in the concentration of serum glucose and that of sodium and potassium respectively. These proportionality factors provide a better theoretical estimation of the osmotic effect caused by hyperglycemia as a function of HbA1c level and considering the action of exogenous insulin and the regulatory mechanisms of the kidney.

Results

In this study, we examined hypovolemia and hyperglycemia induced hyponatremia in DMT1 patients with HbA1c levels ranging from 4.0 to 9.0 using simulation and modeling analysis. We extended the simulation study of Katz to include the effects of the action of insulin and the absorptive capacity of the kidney. Katz's study only looked at the body fluid inter-compartmental volume shift after the infusion of 1000 mOsm of IV glucose bolus in the total absence of insulin and kidney regulation. Normally, patients with DMT1 are managed with exogenous insulin to maintain normal glucose hemostasis. To simulate the effects of hypovolemia on hyperglycemia induced hyponatremia, we examined the effects of the addition of 1000 mOsm of glucose as a bolus IV injection into ECF volume. In our simulation, we included exogenous insulin therapy to

maintain an HbA1c level reflecting the adherence of the patient and the complications of insulin resistance/insufficiency. We simulated insulin resistance/insufficiency by a shifted sigmoid function as described in Section 2.1 and is illustrated in Figure 2. The kidney threshold for glucose clearance is described in Section 2.3 and is illustrated in Figure 3.

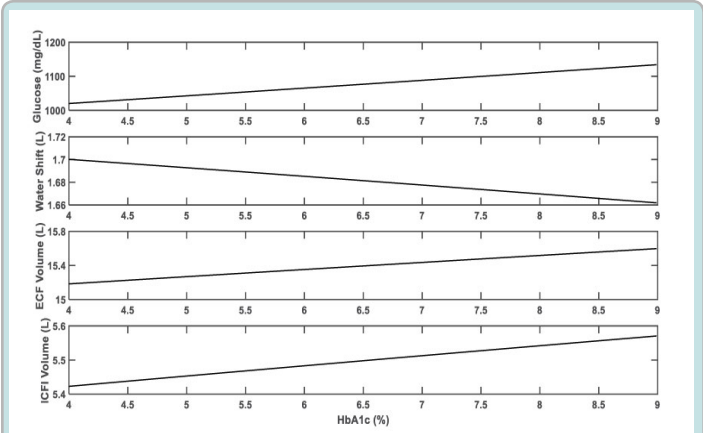


Figure 4: Blood glucose concentration, water shift, extracellular fluid (ECF) and intracellular fluid of insulin insensitive tissues (ICFI) volumes immediately after intravenous (IV) infusion of 1000 mOsm glucose bolus as functions of hemoglobin A1c (HbA1c) level.

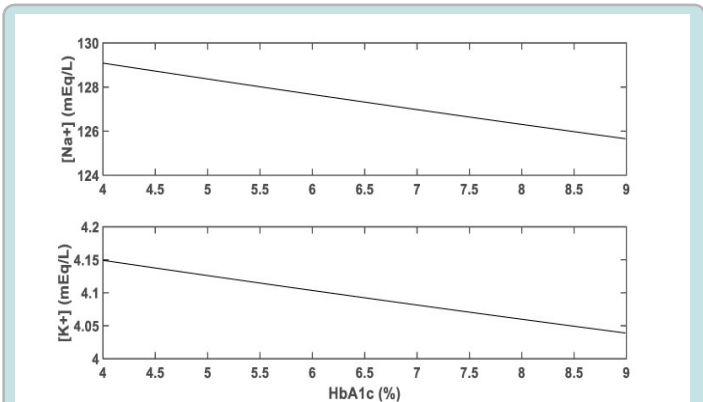


Figure 5: Sodium [Na+] and potassium [K+] concentrations immediately after intravenous (IV) infusion of 1000 mOsm glucose bolus as functions of hemoglobin A1c (HbA1c) level.

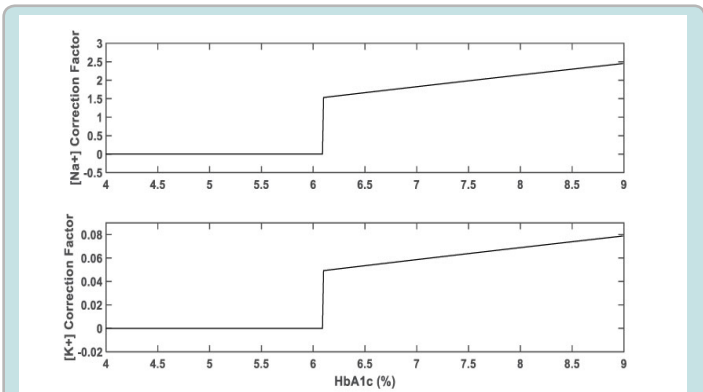


Figure 6: Sodium [Na+] and potassium [K+] concentration correction factors immediately after intravenous (IV) infusion of 1000 mOsm glucose bolus as functions of hemoglobin A1c (HbA1c) level.

Figure 4 illustrates the changes in blood glucose and body fluid compartments volumes immediately after the infusion of 1000 mOsm of IV glucose bolus. Blood glucose concentration increases as HbA1c level increases. At HbA1c level of 9.0 blood glucose exceeded 1200 mg/dL. Both ECF and ICFI volumes increased while ICFS decreased as fluid shifts from ICFS to ECF and ICFI. In particular, ICFI increased from 4.5 (L) to 5.5 (L) at HbA1c level of 9.0. Sodium and Potassium concentrations decreased and reached 126 and 4.0 respectively at HbA1c level of 9.0 as shown in Figure 5. In this acute condition, the patient is severely hyponatremic with a normal potassium level. The correction factors for sodium and potassium concentrations are illustrated in Figure 6. At normal HbA1c levels, the sodium correction factor is close to that estimated by Katz's study. At HbA1c level of 9.0, the sodium correction factor is close to 2.5, which is much higher than that of Katz.

Normally, the rapid increase in blood glucose concentration would induce the secretion of insulin, which in turn allows cells of insulin sensitive tissues to take up glucose. In patients with DMT1, exogenous insulin is injected before or after the ingestion of glucose rich carbohydrates. To simplify the simulation, we assumed that the action of injected insulin would not take place until blood glucose concentration has been stabilized after the infusion of 1000 mOsm of IV glucose bolus. We also assumed that insulin is injected long before the kidney starts excreting excess glucose when blood glucose concentration reaches the absorptive capacity of the kidney. Once insulin dose is injected

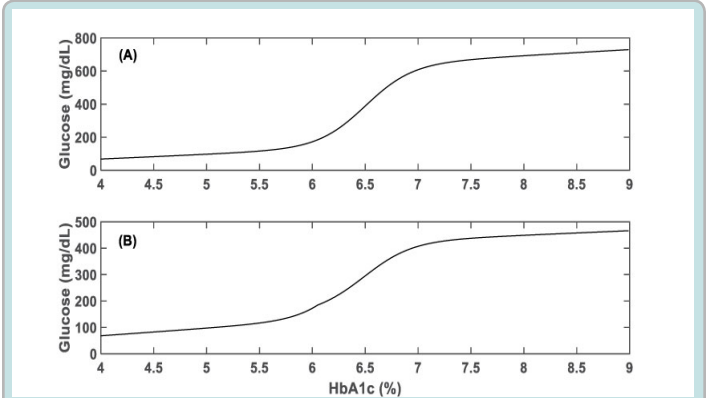


Figure 7: (A) Blood glucose concentrations after insulin action only and (B) after kidney action as functions of hemoglobin A1c (HbA1c) level.

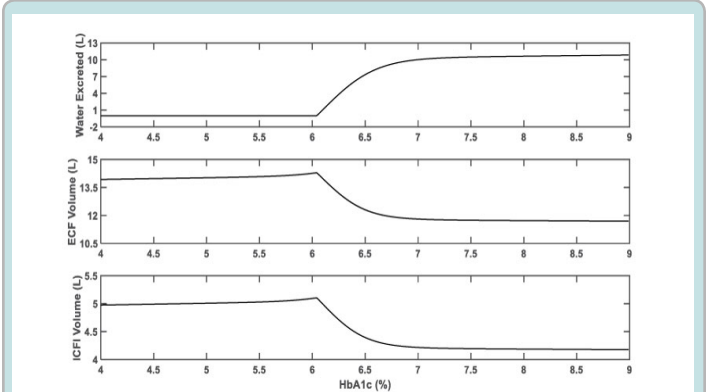


Figure 8: Water shift, extracellular fluid (ECF) and intracellular fluid of insulin insensitive tissues (ICFI) volumes after the action of insulin and the kidney as functions of hemoglobin A1c (HbA1c) level.

at the level necessary to maintain the desired HbA1c level, some glucose is absorbed by insulin sensitive tissues as illustrated in Figure 7(A). From HbA1c level of 4.0 to 6.5, most of the IV infused glucose is absorbed as the insulin dose is sufficient to drive glucose into insulin sensitive tissues. However, as HbA1c level increases, insulin resistance/insufficiency causes excess glucose to accumulate in the blood to as high 750 mg/dL at HbA1c level of 9.0. Figure 7(A) illustrates the action of injected insulin but not the action of the kidney yet.

However, as the blood glucose concentration exceeds the absorptive capacity of the kidney, the kidney starts excreting the excess glucose and attempts to maintain a blood glucose under its threshold capacity as shown in Figure 7(B). At high HbA1c level close to 9.0, the blood glucose concentration reaches 450 mg/dL despite the action of the kidney. However, if the kidney action was allowed to continue beyond the period of simulation, the kidney will ultimately reduce the blood glucose to under the kidney glucose concentration threshold. Regardless of the final glucose accumulation, the action of kidney results in excretion of glucose and associated water due to osmotic effects as shown in Figure 8. The kidney also excretes electrolytes to maintain body osmolarity as normally as possible. Figure 8 illustrates the body fluid compartments volumes redistribution after the action of the kidney. Adjustments to sodium and potassium concentrations are illustrated in Figure 9. Sodium and potassium concentrations decreased to 138 and 4.4 respectively as shown in Figure 9. Although sodium and potassium concentrations decreased, they are still within normal range, which reflects the significant role of

the kidney's action. The excreted sodium and potassium reduce the size of the volume lost. The correction factors for sodium and potassium concentrations after the action of insulin and kidney are illustrated in Figure 10. At normal HbA1c levels, no glucose or water is lost and there is no correction as the exogenous insulin dose is sufficient to maintain homeostasis. However, at HbA1c levels higher than 6.5, water loss is more than sodium and potassium. At HbA1c close to 9.0 sodium concentration must be corrected upwards by a factor close to 5.5 when the steady state glucose concentration doubles.

In this study, we demonstrated that the dynamics of exogenous insulin action and the fluid regulatory mechanisms of the kidney are necessary to control the accumulation of blood glucose and reduce its subsequent effects. In the absence of insulin, continuous diuresis of the kidney due to hyperglycemia can lead to severe complications of hypovolemia. In its simple form, the study of Katz proposed a correction factor for the concentration of sodium during fluid resuscitation for hyperglycemia in patients with DMT1. In the absence of insulin, it may be appropriate to provide fluid administration, because the rationale would suggest that most of the fluid shift to the ECF would ultimately be excreted, and the patient would become hypovolemic. The correction proposed by Katz's study was based only on fluid shift among the body fluid compartments without considering insulin resistance/insufficiency and the effects of kidney regulation. In this study, we included the effects of insulin action and kidney diuresis on electrolytes' concentrations. We showed that not-well-managed or non-compliant patients with DMT1 run the high risk of not only losing fluid but also electrolytes. Consequently, many clinicians worry that the fluid shift from ICFs to ECF and ICFI plus the administration of fluids and electrolytes during resuscitation may cause transient brain edema that may lead to brain injury. A recent study reported that brain injuries are most associated with unbalanced fluid administration during ketoacidosis [64].

Discussion

In this study, we investigated the effects of hypovolemia and hyperglycemia-induced hyponatremia in patients with DMT1. We used a state model to describe the fluid shift among the body fluid compartments due to increased serum glucose. In contrast to Katz's study, we included the action of the exogenous insulin therapy and the regulation of the kidney. To simulate the action of exogenous insulin therapy, we designed a normalized sigmoid function based on Matsuda index to model the functional capacity of the pancreas. Similarly, to simulate the regulation of the kidney, we designed a sigmoid function to represent the kidney glucose threshold as function of the patient's HbA1c level using published data. Our results consist of three main findings. First, without the action of insulin and the kidney, the accumulation of blood glucose reached extremely high levels that may not be manageable without intensive interventions and resuscitation of the patient with high HbA1c level. The sodium concentration drops to levels that can cause significant complications.

Second, the resulting correction factor for the sodium is higher than 1.6 at high HbA1c levels. The action of insulin therapy only did not reduce blood glucose to safe levels. Even with the addition of the action of the kidney blood glucose remained high. The loss of volume and electrolytes is very significant and may lead to fatal hypovolemia. Thus, at high HbA1c levels, fluid resuscitation of the patient is almost necessary to prevent serious

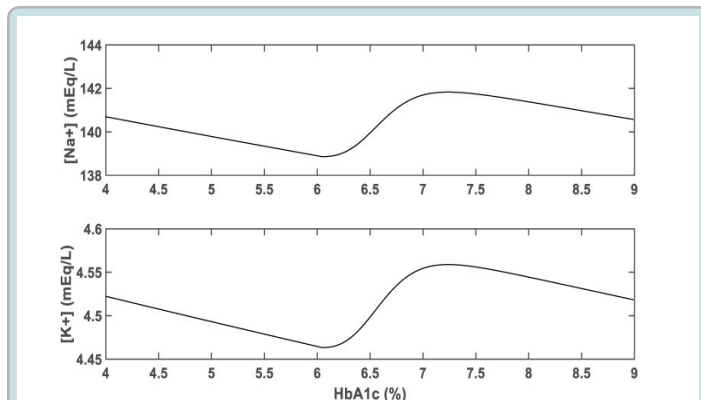


Figure 9: Sodium [Na⁺] and potassium [K⁺] concentrations after the action of insulin and the kidney as functions of hemoglobin A1c (HbA1c) level.

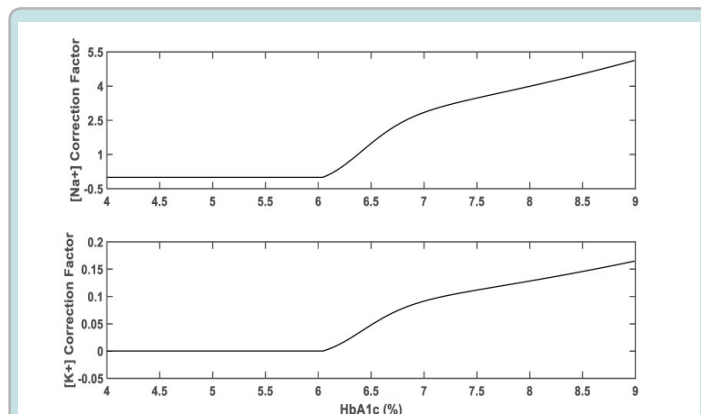


Figure 10: Sodium [Na⁺] and potassium [K⁺] concentration correction factors after the action of insulin and the kidney as functions of hemoglobin A1c (HbA1c) level.

complications, especially those related to the kidney. Third, an interesting finding is the fact that despite the complications that may ensue from the loss of fluid and electrolytes, the measured sodium and potassium concentrations are within normal values. This may lead to confusing interpretation of these values by the clinical staff. This in turn may lead to clinical decisions that may lead to the demise of the patient. In summary, the correction factor of sodium is higher when the action of insulin and kidney are not considered due to the loss of fluid and electrolytes that may be substantial.

Conclusion

We believe that this is the first study to objectively investigate and simulate the changes in serum electrolytes in patients with DMT1 during severe hyperglycemia and ketoacidosis using mathematical concepts of concentration and volume. In this simulation, we demonstrated that serum electrolytes and fluids disturbances can be predicted using state-based modeling and simulation models using a data-based empirical function of insulin resistance/insufficiency at a priori HbA1c level. In emergency conditions, clinical practitioners intervene according to the patient's blood glucose level and vital data of Complete Blood Cell assays (CBC). We selected to use HbA1c level instead of blood glucose level to enhance the outcomes of the simulation. We also demonstrated that the IV injection of glucose bolus causes fluid shift among the body fluid compartments and electrolytes imbalance that may expose the patient with DMT1 to acute and frequent hyponatremic episodes. The fluid shift momentary causes an expansion of ECF and the ICFI fluid compartments, which may acutely affect the brain function if insulin resistance/insufficiency factor is high. However, after rapid glucose metabolism, some of the plasma fluid will be excreted when the kidney absorptive capacity is exceeded. The initial loss of water from the plasma fluid compartment will be redistributed among the body fluid compartments due to the effect of osmosis. Fluid redistribution relatively reduces the effective fluid loss from the plasma fluid compartment, which in turn causes the loss of electrolytes proportionally. The overall loss of fluid not only causes contraction of plasma fluid but also contraction of ICFI fluid. Without the action of insulin and the kidney, the accumulation of blood glucose reached extremely high levels that may not be manageable without intensive interventions and resuscitation of the patient. However, despite the complications that may ensue from the loss of fluid and electrolytes, the measured sodium and potassium concentrations may be within normal values. Hyperglycemia causes electrolytes and fluids disturbances that can be predicted using a statistical driven computer simulation. In summary, this study is a simulation study that investigated the correction factor and demonstrated that the correction factor is much higher than that estimated by Katz's study. We plan to design patient-based clinical studies that will validate the results of this simulation with statistical assessment for clinical decision-making.

Conflicts of Interest Statement

The authors have NO conflict of interest to disclose.

Funding Statement

The authors did NOT receive any funding for this study.

Reference

1. Shaw JE, Sicree RA, Zimmet PZ. (2018). Global estimates of the prevalence of diabetes for 2010 and 2030. *Diabetes Res Clin Pract.* 87: 4-14.
2. Lawrence JM, Divers J, Isom S, Saydah S, Imperatore G, et al. (2021). Trends in Prevalence of Type 1 and Type 2 Diabetes in Children and Adolescents in the US, 2001-2017. *Jama.* 326: 717-727.
3. Mayer-Davis EJ, Lawrence JM, Dabelea D, Divers J, Isom S, et al. (2017). Incidence Trends of Type 1 and Type 2 Diabetes among Youths, 2002-2012. *N Engl J Med.* 376: 1419-1429.
4. Huang ES, Basu A, O'Grady M, Capretta JC. (200). Projecting the future diabetes population size and related costs for the U.S. *Diabetes Care.* 32: 2225-2229.
5. (2018). Economic Costs of Diabetes in the U.S. in 2017. *Diabetes Care.* 41: 917-928.
6. Narayan KM, Boyle JP, Thompson TJ, Sorensen SW, Williamson DF. (2003). Lifetime risk for diabetes mellitus in the United States. *Jama.* 290: 1884-1890.
7. Ioacara S, Lichiardopol R, Ionescu-Tirgoviste C, Cheta D, Sabau S, et al. (2009). Improvements in life expectancy in type 1 diabetes patients in the last six decades. *Diabetes Res Clin Pract.* 86: 146-151.
8. Secrest AM, Becker DJ, Kelsey SF, LaPorte RE, Orchard TJ. (2010). All-cause mortality trends in a large population-based cohort with long-standing childhood-onset type 1 diabetes: the Allegheny County type 1 diabetes registry. *Diabetes Care.* 33: 2573-2579.
9. Roep BO. (2003). The role of T-cells in the pathogenesis of Type 1 diabetes: from cause to cure. *Diabetologia.* 46: 305-321.
10. Eizirik DL, Colli ML, Ortis F. (2009). The role of inflammation in insulinitis and beta-cell loss in type 1 diabetes. *Nat Rev Endocrinol.* 5: 219-226.
11. Willcox A, Richardson SJ, Bone AJ, Foulis AK, Morgan NG. (2009). Analysis of islet inflammation in human type 1 diabetes. *Clin Exp Immunol.* 155: 173-81.
12. Singleton JR, Smith AG, Bromberg MB. (2001). Increased prevalence of impaired glucose tolerance in patients with painful sensory neuropathy. *Diabetes Care.* 24: 1448-1453.
13. Biessels GJ, Staekenborg S, Brunner E, Brayne C, Scheltens P. (2006). Risk of dementia in diabetes mellitus: a systematic review. *Lancet Neurol.* 5: 64-74.
14. Callaghan BC, Cheng HT, Stables CL, Smith AL, Feldman EL. (2012). Diabetic neuropathy: clinical manifestations and current treatments. *Lancet Neurol.* 11: 521-534.
15. Asghar O, Petropoulos IN, Alam U, Jones W, Jeziorska M, et al. (2014). Corneal confocal microscopy detects neuropathy in subjects with impaired glucose tolerance. *Diabetes Care.* 37: 2643-2646.
16. Cameron FJ, Scratch SE, Nadebaum C, Northam EA, Koves I, et al. (2014). Neurological consequences of diabetic ketoacidosis at initial presentation of type 1 diabetes in a prospective cohort study of children. *Diabetes Care.* 37: 1554-1562.
17. Cato MA, Mauras N, Mazaika P, Kollman C, Cheng P, et al. (2016). Longitudinal Evaluation of Cognitive Functioning in Young Children with Type 1 Diabetes over 18 Months. *J Int Neuropsychol Soc.* 22: 293-302.

18. Castelli G, Desai KM, Cantone RE. (2020). Peripheral Neuropathy: Evaluation and Differential Diagnosis. *Am Fam Physician*. 102: 732-739.
19. Faselis C, Katsimardou A, Imprialos K, Deligkaris P, Kallistratos M, et al. (2020). Microvascular Complications of Type 2 Diabetes Mellitus. *Curr Vasc Pharmacol*. 18: 117-124.
20. Harjutsalo V, Thomas MC, Forsblom C, Groop PH. (2018). Risk of coronary artery disease and stroke according to sex and presence of diabetic nephropathy in type 1 diabetes. *Diabetes Obes Metab*. 20: 2759-2767.
21. Edge JA, Hawkins MM, Winter DL, Dunger DB. (2001). The risk and outcome of cerebral oedema developing during diabetic ketoacidosis. *Arch Dis Child*. 85: 16-22.
22. Glaser N, Barnett P, McCaslin I, Nelson D, Trainor J, et al. (2001). Risk factors for cerebral edema in children with diabetic ketoacidosis. The Pediatric Emergency Medicine Collaborative Research Committee of the American Academy of Pediatrics. *N Engl J Med*. 344: 264-269.
23. Bohn D, Daneman D. (2002). Diabetic ketoacidosis and cerebral edema. *Curr Opin Pediatr*. Jun 14: 287-291.
24. Levitsky LL. (2004). Symptomatic cerebral edema in diabetic ketoacidosis: the mechanism is clarified but still far from clear. *J Pediatr*. 145: 149-150.
25. Muir AB, Quisling RG, Yang MC, Rosenbloom AL. (2004). Cerebral edema in childhood diabetic ketoacidosis: natural history, radiographic findings, and early identification. *Diabetes Care*. 27: 1541-1546.
26. Close TE, Cepinskas G, Omatsu T, Rose KL, Summers K, et al. (2013). Diabetic ketoacidosis elicits systemic inflammation associated with cerebrovascular endothelial cell dysfunction. *Microcirculation*. Aug 20: 534-543.
27. Mahoney CP, Vlcek BW, DelAguila M. (1999). Risk factors for developing brain herniation during diabetic ketoacidosis. *Pediatr Neurol*. 21: 721-727.
28. Wang J, Williams DE, Narayan KM, Geiss LS. (2006). Declining death rates from hyperglycemic crisis among adults with diabetes, U.S., 1985-2002. *Diabetes Care*. 29: 2018-2022.
29. Fritsch M, Rosenbauer J, Schober E, Neu A, Placzek K, et al. (2011). Predictors of diabetic ketoacidosis in children and adolescents with type 1 diabetes. Experience from a large multicentre database. *Pediatr Diabetes*. 12: 307-312.
30. Milionis HJ, Lيامis G, Elisaf MS. (2001). Appropriate treatment of hypernatraemia in diabetic hyperglycaemic hyperosmolar syndrome. *J Intern Med*. 249: 273-276.
31. Kitabchi AE, Umpierrez GE, Miles JM, Fisher JN. (2009). Hyperglycemic crises in adult patients with diabetes. *Diabetes Care*. 32: 1335-1343.
32. Lيامis G, Liberopoulos E, Barkas F, Elisaf M. (2014). Diabetes mellitus and electrolyte disorders. *World J Clin Cases*. 2: 488-496.
33. Tzamaloukas AH, Rohrscheib M, Ing TS, Siamopoulos KC, Elisaf MF, et al. (2004). Serum tonicity, extracellular volume and clinical manifestations in symptomatic dialysis-associated hyperglycemia treated only with insulin. *Int J Artif Organs*. 27: 751-758.
34. Wilinska ME, Bodenlenz M, Chassin LJ, Schaller HC, Schaupp LA, et al. (2004). Interstitial glucose kinetics in subjects with type 1 diabetes under physiologic conditions. *Metabolism*. 53: 1484-1491.
35. Rose AJ, Richter EA. (2005). Skeletal muscle glucose uptake during exercise: how is it regulated? *Physiology (Bethesda)*. 20: 260-270.
36. Steil GM, Rebrin K, Hariri F, et al. (2005). Interstitial fluid glucose dynamics during insulin-induced hypoglycaemia. *Diabetologia*. 48: 1833-1840.
37. Moran SM, Jamison RL. (1985). The variable hyponatremic response to hyperglycemia. *West J Med*. 14: 49-53.
38. Tzamaloukas AH, Ing TS, Siamopoulos KC, Rohrscheib M, Elisaf MS, et al. (2008). Body fluid abnormalities in severe hyperglycemia in patients on chronic dialysis: review of published reports. *J Diabetes Complications*. 22: 29-37.
39. DeFronzo RA, Davidson JA, Del Prato S. (2012). The role of the kidneys in glucose homeostasis: a new path towards normalizing glycaemia. *Diabetes Obes Metab*. 14: 5-14.
40. Rondon-Berrios H, Argyropoulos C, Ing TS, et al. (2017). Hypertonicity: Clinical entities, manifestations and treatment. *World J Nephrol*. 6: 1-13.
41. Hillier TA, Abbott RD, Barrett EJ. (1999). Hyponatremia: evaluating the correction factor for hyperglycemia. *Am J Med*. 106: 399-403.
42. Katz MA. (1973). Hyperglycemia-induced hyponatremia--calculation of expected serum sodium depression. *N Engl J Med*. 289: 843-844.
43. Roscoe JM, Halperin ML, Rolleston FS, Goldstein MB. (1975). Hyperglycemia-induced hyponatremia: metabolic considerations in calculation of serum sodium depression. *Can Med Assoc J*. 112: 452-453.
44. Evans LE, Taylor JL, Smith CJ, Pritchard HAT, Greenstein AS, et al. (2021). Cardiovascular comorbidities, inflammation, and cerebral small vessel disease. *Cardiovasc Res*. 117: 2575-2588.
45. Liu J, Rutten-Jacobs L, Liu M, Markus HS, Traylor M. (2018). Causal Impact of Type 2 Diabetes Mellitus on Cerebral Small Vessel Disease: A Mendelian Randomization Analysis. *Stroke*. Jun 49: 1325-1331.
46. Forbes JM, Cooper ME. (2013). Mechanisms of diabetic complications. *Physiol Rev*. 93: 137-188.
47. Castellanos L, Tuffaha M, Koren D, Levitsky LL. (2020). Management of Diabetic Ketoacidosis in Children and Adolescents with Type 1 Diabetes Mellitus. *Paediatr Drugs*. 22: 357-367.
48. Westerberg DP. (2013). Diabetic ketoacidosis: evaluation and treatment. *Am Fam Physician*. 87: 337-346.
49. Diringier M. (2017). Neurologic manifestations of major electrolyte abnormalities. *Handb Clin Neurol*. 141: 705-713.
50. Hobbs N, Samadi S, Rashid M, et al. (2022). A physical activity-intensity driven glycemic model for type 1 diabetes. *Comput Methods Programs Biomed*. 226: 107153.
51. Rashid M, Samadi S, Sevil M, et al. (2019). Simulation Software for Assessment of Nonlinear and Adaptive Multivariable Control Algorithms: Glucose - Insulin Dynamics in Type 1 Diabetes. *Comput Chem Eng*. 130.

52. Man CD, Micheletto F, Lv D, Breton M, Kovatchev B, et al. (2014). The UVA/PADOVA Type 1 Diabetes Simulator: New Features. *J Diabetes Sci Technol*. 8: 26-34.
53. Matsuda M, DeFronzo RA. (1999). Insulin sensitivity indices obtained from oral glucose tolerance testing: comparison with the euglycemic insulin clamp. *Diabetes Care*. 22: 1462-1470.
54. Gastaldelli A, Ferrannini E, Miyazaki Y, Matsuda M, DeFronzo RA. (2004). Beta-cell dysfunction and glucose intolerance: results from the San Antonio metabolism (SAM) study. *Diabetologia*. 47: 31-39.
55. Godsland IF, Jeffs JAR, Johnston DG. (2004). Loss of beta cell function as fasting glucose increases in the non-diabetic range. *Diabetologia*. 47: 1157-1166.
56. Ferrannini E, Gastaldelli A, Miyazaki Y, Matsuda M, Mari A, DeFronzo RA. (2005). beta-Cell function in subjects spanning the range from normal glucose tolerance to overt diabetes: a new analysis. *J Clin Endocrinol Metab*. 90: 493-500.
57. Kanat M, Winnier D, Norton L, Arar N, Jenkinson C, et al. (2011). The relationship between {beta}-cell function and glycated hemoglobin: results from the veterans administration genetic epidemiology study. *Diabetes Care*. 34: 1006-1010.
58. Kyurkchiev N, Markov S. (2015). Sigmoid Functions Some Approximation and Modelling Aspects: Some Moduli in Programming Environment MATHEMATICA.
59. Marquardt DW, duPont EI, RB, Burrell GC. Marquardt DW. (1963). An algorithm for least-squares estimation of nonlinear parameters. *J Soc Indust Appl. Math*. 11: 431-441.
60. Chen Z, Cao F. (2009). The approximation operators with sigmoidal functions. *Comput Math Appl*. 58: 758-765.
61. Osaki A, Okada S, Saito T, Yamada E, Ono K, et al. (2016). Renal threshold for glucose reabsorption predicts diabetes improvement by sodium-glucose cotransporter 2 inhibitor therapy. *J Diabetes Investig*. 7: 751-754.
62. Yue XD, Wang JY, Zhang XR, Yang JH, Shan CY, et al. Characteristics and Impact Factors of Renal Threshold for Glucose Excretion in Patients with Type 2 Diabetes Mellitus. *J Korean Med Sci*. 32: 621-627.
63. Hieshima K, Sugiyama S, Yoshida A, Kurinami N, Suzuki T, et al. (2020). Elevation of the renal threshold for glucose is associated with insulin resistance and higher glycated hemoglobin levels. *J Diabetes Investig*. 11: 617-625.
64. Badawi NES, Hafez M, Eldin HS, et al. (2021). Outcome of the use of 0.9% saline versus 0.45% saline for fluid rehydration in moderate and severe diabetic ketoacidosis in children. *Egyptian Pediatric Association Gazette*. 69: 10.